

ChemComm

Accepted Manuscript



This is an *Accepted Manuscript*, which has been through the Royal Society of Chemistry peer review process and has been accepted for publication.

Accepted Manuscripts are published online shortly after acceptance, before technical editing, formatting and proof reading. Using this free service, authors can make their results available to the community, in citable form, before we publish the edited article. We will replace this *Accepted Manuscript* with the edited and formatted *Advance Article* as soon as it is available.

You can find more information about *Accepted Manuscripts* in the [Information for Authors](#).

Please note that technical editing may introduce minor changes to the text and/or graphics, which may alter content. The journal's standard [Terms & Conditions](#) and the [Ethical guidelines](#) still apply. In no event shall the Royal Society of Chemistry be held responsible for any errors or omissions in this *Accepted Manuscript* or any consequences arising from the use of any information it contains.

Cite this: DOI: 10.1039/c0xx00000x

www.rsc.org/xxxxxx

ARTICLE TYPE

Mono-Benzimidazole Functionalized β -Cyclodextrins as Supramolecular Nanovalves for pH-Triggered Release of *p*-Coumaric Acid

Ting Wang,[‡] MingDong Wang,[‡] ChenDi Ding and JiaJun Fu^{*}

Received (in XXX, XXX) Xth XXXXXXXXXX 20XX, Accepted Xth XXXXXXXXXX 20XX

DOI: 10.1039/b000000x

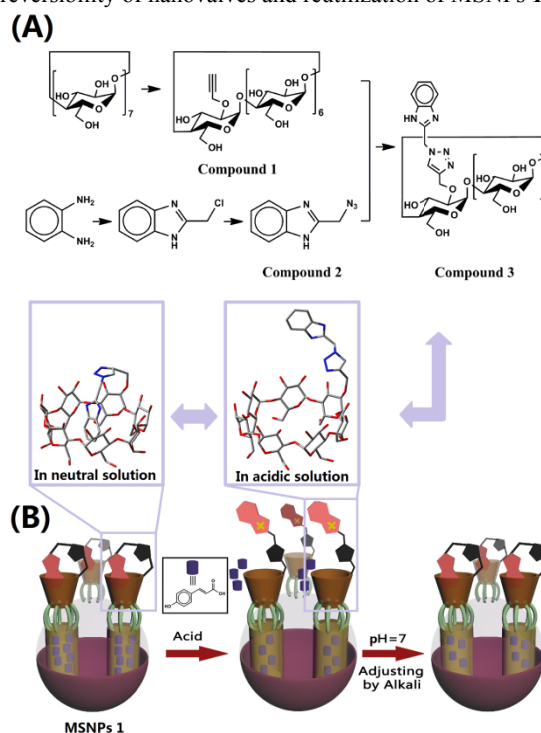
The self-complexation of mono-benzimidazole functionalized β -cyclodextrins was investigated. The unique molecular structure employed as supramolecular nanovalves were installed on external surface of mesoporous silica to assemble mechanized silica nanoparticles, which show the pH-triggered release property.

Nanovalves, as the important category of molecular machines, are capable of achieving effectiveness of valves at molecular dimensions and control the flow of cargo molecules precisely.¹ Nanovalves reversibly transform from “open” states to “closed” states by changing molecular configurations or chemical bonding models, which results from the environmental stimuli, such as pH, temperature, redox, enzyme, and light.²

In recent decades, with the in-depth research of supramolecular chemistry, mechanically interlocked molecules, including bistable [2] catenanes, bistable [2] rotaxanes as well as pseudorotaxanes, are employed as supramolecular nanovalves to construct mechanized silica nanoparticles (MSNPs) and are responsible for accomplishing controlled release tasks, relying on the fact that strength of non-covalent interactions between two key components of nanovalves, stalks and macrocycles can be tuned by the external forces.³ Compared with the other traditional type of stimuli-responsive polymeric nanovalves, the MSNPs based on the mesoporous silica nanoparticles (MSNs) as scaffolds have their own merits, such as tunable particle size, high loading capacity, negligible premature cargo leakage, sustainable release property and show the advantages in the tumor-targeted drug delivery and smart anticorrosion coatings.⁴ Unlike molecular nanovalves with the attribute of reversibility, supramolecular nanovalves are mostly irreversible upon activation, especially for [2] pseudorotaxanes. After release processes, the macrocycles, such as cyclodextrin, cucurbituril, pillararenes, *etc.* dethread from the functional stalks and the integrated structure of [2] pseudorotaxanes are destroyed.⁵ In comparison, bistable [2] rotaxanes are more adaptable to be used as nanovalves. The reciprocating motions of macrocycles between two recognition sites upon stimuli execute the mission of “release-stop-release”.⁶ However, their preparations usually require multiple steps and are time-consuming.

The mono-functionalized macrocycles, mainly concentrating in cyclodextrin and pillararene due to their easily decorated structures have exhibited the distinctive self-complexation property in dilute solution.⁷ To our knowledge, there have been

no reports on the usage of self-complexation structure as supramolecular nanovalves so far. Herein, we envisage and prepare the mono-benzimidazole functionalized β -cyclodextrins by the introduction of 1*H*-benzimidazole (BZI) group at the secondary side of β -cyclodextrin (β -CD) via 1,3-dipolar cycloaddition reaction (Scheme 1A). Then the mono-BZI functionalized β -CD as supramolecular nanovalves are installed on the surface of MSNs to assemble MSNPs **1**. In the neutral solution, BZI groups get into the cavity of β -CD, forming self-complexation structure and blocking the diffusion channels. While in the acidic solution, BZI groups are protonated, the binding constant between BZI and β -CD decreases dramatically,⁸ which results in the ejection of BZI groups. At this moment, the nanovalves are opened and cargo molecules can diffuse out through the cavities of β -CD (Scheme 1B). Benefiting from self-switched characteristic, the hosts “ β -CD” and the guests “BZI” are linked by triazole rings, which guarantees great probability for reversibility of nanovalves and reutilization of MSNPs **1**.



Scheme 1. (A) Synthesis Route of Compound 3; (B) Working mechanism of MSNPs 1.

For the construction of mono-BZI functionalized β -CD, we decided to carry out the synthesis of mono-2-O-[1-(1*H*-benzimidazol-2-ylmethyl)-1*H*-[1,2,3] triazol-4-ylmethyl]- β -cyclodextrin (Compound **3**, Scheme 1A). We first synthesize mono-2-O-propargyl- β -cyclodextrin (Compound **1**) in a facile route. Taking advantage of terminal alkyne group linked to the O2 position, Cu (I)-catalyzed azide-alkyne Huisgen cycloaddition reactions of Compound **1** was performed with 2-(azidomethyl)-1*H*-benzimidazole (Compound **2**), which was obtained *via* nucleophilic substitution by using sodium azido solution, to afford the click product Compound **3** (the detailed synthesis process can be seen in ESI†, Scheme S1-S3, Fig. S1-S3). The self-complexation behaviour of Compound **3** was first investigated by ^1H NMR spectroscopy. The concentration of Compound **3** is below 0.1 mM in order to avoid intermolecular self-assembly.⁷ The ^1H NMR spectrum of Compound **3** in D_2O is shown in Fig. 1A. Upon addition of 1 equiv. of DCl (Fig. 1B), the peaks for BZI (H_a , H_b) display the substantial downfield shifts ($\Delta\delta_a=0.20$, $\Delta\delta_b=0.37$ ppm) and a strong spectral simplification of the β -CD region is observed. After adjusting to neutral solution by NaOD, the signals of H_a , H_b as well as H-3 and H-5 (marked in Scheme S1, ESI†), which locate inside the cavity of β -CD shift remarkably upfield. The cyclic process from Fig.1 indicates the self-inclusion of the BZI moiety into the hydrophobic β -CD cavity in neutral solution and the dethreading occurs under acidic environment. The pH-dependent spatial conformation of Compound **3** can be further confirmed by 2D ROESY (Fig. S4, ESI†). From 2D ROESY analysis, ROE correlations are observed between protons of BZI and protons of β -CD at neutral pH and disappear in the acidic condition. Further evidence for supporting switchable action was obtained by UV-vis measurements (Fig S5, ESI†).

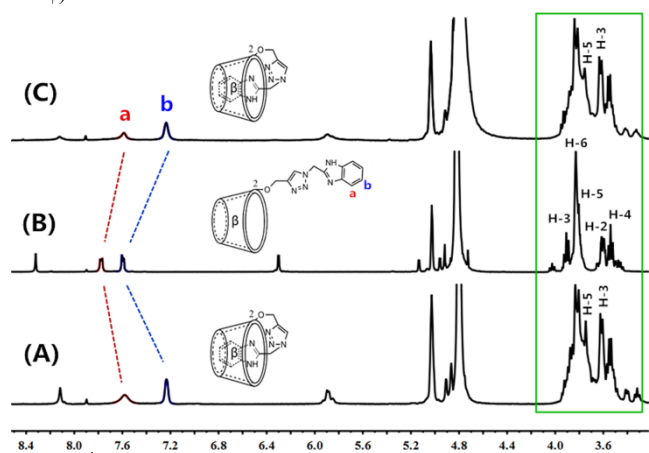


Fig. 1. ^1H NMR spectra of Compound **3** in D_2O : (A) at 25 °C; (B) adding 1.0 equiv. DCl; (C) adding 1.0 equiv. NaOD.

MCM-41-type MSNs with an average diameter of 150 nm, specific surface are of $1000.82\text{ m}^2\text{ g}^{-1}$ and pore size of 2.29 nm were synthesized according to a previously reported method (Figure S6, ESI†).⁹ The hexagonally arranged pores of the MSNs, which will accommodate cargo molecules were analysed through transmission electron microscopy (TEM) and small-angle X-ray diffraction (SA-XRD). The synthesis route of MSNPs **1** is shown in Scheme S6 (ESI†). Initially, the MSNs used as inorganic scaffold were reacted with (3-aminopropyl) trimethoxysilane

(APTES) to obtain MSNs-NH₂. Subsequently, in order to facilitate supramolecular nanovalves (Compound **3**) to attach the MSNs-NH₂, heptakis (6-deoxy-6-iodo) modified Compound **3** was prepared (Compound **4**, synthesis process is in ESI†). Next, Compound **4** was covalently anchored onto the external surface of MSNs through nucleophilic substitution reaction to afford MSNs-CD-BZI. Finally, the adsorption of *p*-coumaric acid as cargo molecules and the closure of supramolecular nanovalves were accomplished by precisely adjusting pH values of solution, and then MSNPs **1** were assembled.

FTIR spectra (Figure S7, ESI†) were used to characterize two-steps functionalization process of MSNs. Compared with the Si-O-Si stretching (1080 cm^{-1}), Si-OH stretching (3434 cm^{-1}) and bending vibrations (1621 cm^{-1}) of bare MSNs, the new peaks at 2933 and 2856 cm^{-1} in the MSNs-NH₂ are due to the asymmetric and symmetric C-H stretching vibrations, and the 3078 cm^{-1} weak peak is ascribed to the N-H stretching vibration. Upon functionalization with Compound **4**, the appearance of peaks at 1539, 1452 and 1386 cm^{-1} are assigned the characteristic of benzene rings, C=N stretching and C-N stretching vibration in BZI rings, respectively, which indicates the successful attachment of supramolecular nanovalves. The grafting of the different functional groups onto the surface of MSNs was further confirmed by the solid-state ^{13}C and ^{29}Si CP/MAS NMR spectra as depicted in Fig. 2. The NMR spectrum of MSNs-NH₂ shows three resonance signals at about 38, 18 and 5 ppm, which are assigned to characteristic carbon peaks of i, j, k on 3-aminopropyl groups. In the NMR spectrum of MSNs-CD-BZI, apart from the peaks of carbons i', j', k', a series of new signals are clearly observed owing to the resonances of nanovalves. The additional resonances are divided into two regions: (i) the signals at 97, 78, 68 and 52 ppm correspond to the carbon peaks of C₁, C₄, C_{2/3/5} and C₆ on the β -CD, respectively; (ii) the signals at the range of 158~125 ppm are attributed to the characteristic carbon peaks on BZI groups. Additionally, the ^{29}Si spectrum of MSNs-CD-BZI reveals bulk silicon peaks (Q region) around $-124\sim-90$ ppm and T type signals (T region) at about $-84\sim-61$ ppm, confirming the functionalized silica resonances. The zeta potentials for MSNs, MSNs-NH₂ and MSNs-CD-BZI at pH 7.0 are -22.5 , $+7.5$ and $+1.9$ mV, respectively. This changing tendency also supports that the two-step functionalization proceeds smoothly.

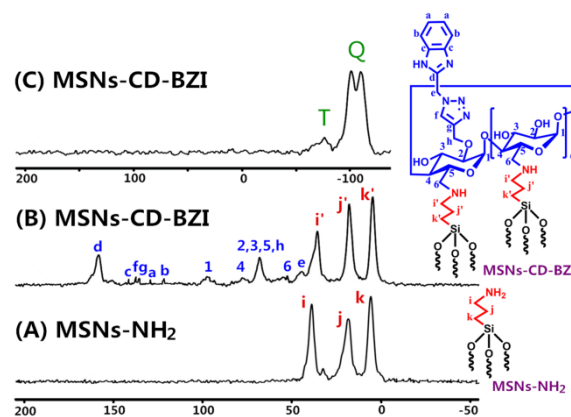


Fig. 2. ^{13}C CP-MAS solid-state NMR spectra of (A) MSNs-NH₂; (B) MSNs-CD-BZI and (C) ^{29}Si CP-MAS NMR spectrum of MSN-CD-BZI.

The grafting contents of APTES and Compound **3** onto MSNs were determined by thermogravimetric analysis to be approximately 1.457 and 0.15 mmol/g MSNs, respectively (Fig. S8, ESI†). Based on the calculation method proposed by Zhao *et al.*,¹⁰ one mesopore is capped with one supramolecular nanovalve under ideal conditions through seven C-N bonds as illustrated in Scheme 1B. Therefore, the roughly estimated grafting efficiency seems satisfactory. The MSNs-NH₂ and MSNs-CD-BZI exhibit certain decrease in the specific surface area, pore volume, as well as pore size, which can be attributed to the partial occupation of pore channel of the stalks (Fig. S9 and Table S2, ESI†). However, through careful analysis SA-XRD patterns (Fig. S10, ESI†) and TEM images (Fig. S11, ESI†), it can be concluded that after functionalization, MSNs-CD-BZI maintain the hexagonal mesoporous structure, which is beneficial for the subsequent adsorption of cargo molecules.

In order to facilitate *p*-coumaric acid to diffuse into MSNs-CD-BZI, the loading process was performed in acidic solution under 60 °C. Acidic environment ensures that the nanovalves are on the open state, and the thermal effect accelerates the self-decomplexation rate thus enhances the adsorption capacity. After 48 h, the pH of solution was gradually adjusted to neutral and the solution was cooled to room temperature simultaneously, MSNPs **1** were collected for release experiments. To investigate the pH-dependent gating effect, MSNPs **1** were placed at various pH values, and the release amount of *p*-coumaric acid was determined by the measurements of fluorescence intensity at 439 nm ($\lambda_{\text{exc}}=351$ nm), which was converted to corresponding concentration according to the standard curve generated automatically by spectrophotometer. As shown in Fig. 3, under neutral pH, almost no release was noticed because the pore outlets were blocked by the nanovalves. Upon turning the pH to acidity, the sustained-release was detected, with approximately 32%, 47% and 76% of the cargo molecules released within 400 min at pH 5.0, 4.0 and 3.0, respectively. These imply that the self-decomplexation between BZI and β -CD under acidic solution and the nanovalves are open to *p*-coumaric acid. The release rate is significantly accelerated with decreasing pH value. When the solution pH value is below 6.0, the protonation of the BZI moiety (pK_a value of 5.68) occurs, resulting in the significant decrease of binding affinity, dissociation of BZI from β -CD and thus destruction of the original stable self-complexation structure (under pH 7.0).¹¹ The stronger the acidity is, the higher degree of the protonation of BZI groups, and the more entrances are open to

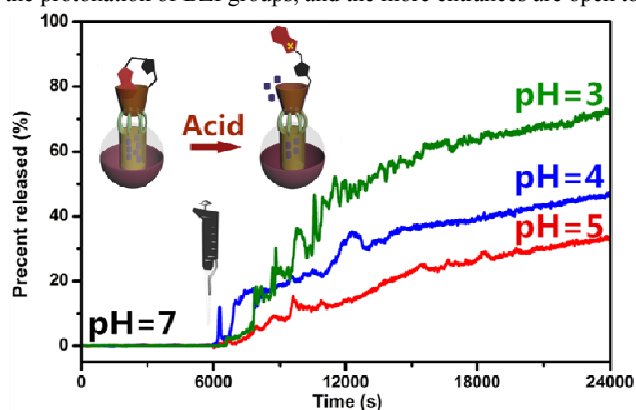


Fig. 3. Release profiles of MSNPs **1** at different pH values.

release cargo molecules. A series of control experiments were performed to corroborate the switching function of supramolecular nanovalves. As Fig. S12 shows, MSNs-CD (MSNs functionalized with heptakis (6-deoxy-6-iodo)- β -CD and no BZI groups linked through O2 position) did not demonstrate pH-controlled release property, evidencing the central role of the mono-BZI functionalized β -CD in the working mechanism.

Furthermore, according to our conception, the self-complexation/decomplexation between β -CD and BZI makes the supramolecular nanovalves operate reversibly. To demonstrate their reversibility, MSNPs **1** were immersed in solution in which the pH of the solution was carefully adjusted as the route of “neutral-acidic-neutral-acidic”, and the staged release profile is shown in Fig. 4. As expected, the states of nanovalves depended on the pH values, and the release of cargo molecules was triggered by the addition of acid and shut off in the neutral solution. It is worthwhile to note that when the pH changed from acidic to neutral, the MSNPs **1** took short time to reach equilibrium and the nanovalves quickly closed again to inhibit the flow out of cargo molecules.

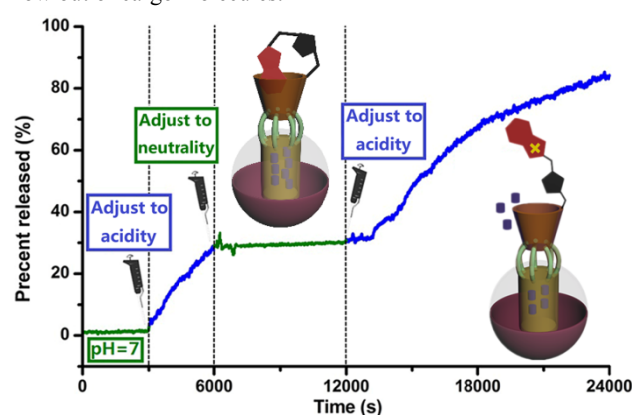


Fig. 4. Staged release profile of MSNPs **1**.

In summary, we have successfully assembled MSNPs **1** based on the mono-BZI functionalized β -CD as supramolecular nanovalves, which show the pH-triggered release character and maintain the reversibility of the nanovalves. Studies are ongoing to investigate their performance of cellular targeted drug delivery and construct the multi-stimuli responsive systems on the basis of self-complexation systems.

This research was financially supported by the National Natural Science Foundation of China (No. 51102135), the Natural Science Foundation of Jiangsu Province (No. BK2011711), the 2013-ZiJin-0102 Talent Program, NUST and QingLan Project, Jiangsu Province, China.

Notes and references

⁹⁵ School of Chemical Engineering, Nanjing University of Science and Technology, Nanjing, China. Fax: +86 025 84315609; Tel: +86 025 84315609; E-mail: fujiacun668@gmail.com

† Electronic Supplementary Information (ESI) available: [Experimental details and analytical data]. See DOI: 10.1039/b000000x/

⁹⁰ ‡ These authors contributed equally to this article.

1. (a) S. Mura, J. Nicolas, P. Couvreur, *Nat. Mater.*, 2013, **12**, 991; (b) S. Saha, K. C. F. Leung, T. D. Nguyen, J. F. Stoddart and J. I. Zink, *Adv. Funct. Mater.*, 2007, **17**, 685; (c) S. Angelos, E. Johansson, J. F. Stoddart and J. I. Zink, *Adv. Funct.*

- Mater.*, 2007, **17**, 2261; (d) M. M. Boyle, R. A. Smaldone, A. C. Whalley, M. W. Ambrogio, Y. Y. Botros and J. F. Stoddart, *Chem. Sci.*, 2011, **2**, 204.
- 2.(a) T. Chen, N. W. Yang and J. J. Fu, *Chem. Commun.*, 2013, **49**, 6555; (b) X. Ma, K. T. Nguyen, P. Borah, C. Y. Ang and Y. L. Zhao, *Adv. Healthc. Mater.*, 2012, **1**, 690; (c) Y. L. Sun, Y. Zhou, Q. L. Li and Y. W. Yang, *Chem. Commun.*, 2013, **49**, 9033; (d) D. P. Ferris, Y. L. Zhao, N. M. Khashab, H. A. Khatib, J. F. Stoddart and J. I. Zink, *J. Am. Chem. Soc.*, 2009, **131**, 1686; (e) J. Croissant and J. I. Zink, *J. Am. Chem. Soc.*, 2012, **134**, 7628; (f) Y. L. Sun, B. J. Yang, S. X. A. Zhang and Y. W. Yang, *Chem.-Eur. J.*, 2012, **18**, 9212; (g) Y. Zhou, L. L. Tan, Q. L. Li, X. L. Qiu, A. D. Qi, Y. C. Tao and Y. W. Yang, *Chem.-Eur. J.*, 2014, **20**, 2998.
- 15 3.(a) M. W. Ambrogio, C. R. Thomas, Y. L. Zhao, J. I. Zink and J. F. Stoddart, *Accounts Chem. Res.*, 2011, **44**, 903; (b) P. P. Yang, S. L. Gai and J. Lin, *Chem. Soc. Rev.*, 2012, **41**, 3679; (c) Y. W. Yang, *Med. Chem. Comm.*, 2011, **2**, 1033. (d) Y. W. Yang, Y. L. Sun and N. Song, *Accounts Chem. Res.*, 2014, **47**, 1950; (e) Y. L. Sun, Y. W. Yang, D. X. Chen, G. Wang, Y. Zhou, C. Y. Wang and J. F. Stoddart, *Small*, **9**, 3224.
- 4.(a) A. Popat, S. B. Hartono, F. Stahr, J. Liu, S. Z. Qiao and G. Q. Lu, *Nanoscale*, 2011, **3**, 2801; (b) J. J. Fu, T. Chen, M. D. Wang, N. W. Yang, S. N. Li, Y. Wang and X. D. Liu, *ACS Nano*, 2013, **7**, 11397; (c) T. Chen and J. J. Fu, *Nanotechnology*, 2012, **23**, 505705.
- 5.(a) L. Du, S. J. Liao, H. A. Khatib, J. F. Stoddart and J. I. Zink, *J. Am. Chem. Soc.*, 2009, **131**, 15136; (b) S. Angelos, Y. W. Yang, K. Patel, J. F. Stoddart and J. I. Zink, *Angew. Chem. Int. Edit.*, 2008, **47**, 2222.
- 30 6.(a) T. D. Nguyen, H. R. Tseng, P. C. Celestre, A. H. Flood, Y. Liu, J. F. Stoddart and J. I. Zink, *Proc. Natl Acad. Sci. USA*, 2005, **102**, 10029; (b) H. Yan, C. Teh, S. Sreejith, L. L. Zhu, A. Kwok, W. Q. Fang, X. Ma, K. T. Nguyen, V. Korzh and Y. L. Zhao, *Angew. Chem. Int. Edit.*, 2012, **51**, 8373; (c) M. D. Wang, T. Chen, C. D. Ding and J. J. Fu, *Chem. Commun.*, 2014, **50**, 5068; (d) H. Li, L. L. Tan, P. Jia, Q. L. Li, Y. L. Sun, J. Zhang, Y. Q. Ning, J. H. Yu and Y. W. Yang, *Chem. Sci.*, 2014, **5**, 2804;
- 40 7.(a) M. Becuwe, F. Cazier, M. Bria, P. Woisel and F. Delattre, *Tetrahedron Lett.*, 2007, **48**, 6186; (b) Z. B. Zhang, Y. Luo, J. Z. Chen, S. Y. Dong, Y. H. Yu, Z. Ma and F. H. Huang, *Angew. Chem. Int. Edit.*, 2011, **50**, 1397; (c) N. L. Strutt, H. C. Zhang, M. A. Giesener, J. Y. Lei and J. F. Stoddart, *Chem Commun.*, 2012, **48**, 1647.
- 45 8.(a) M. Xue, X. Zhong, Z. Shaposhnik, Y. Q. Qu, F. Tamanoi, X. F. Duan and J. I. Zink, *J. Am. Chem. Soc.*, 2011, **133**, 8798; (b) H. A. Meng, M. Xue, T. A. Xia, Y. L. Zhao, F. Tamanoi, J. F. Stoddart, J. I. Zink and A. E. Nel, *J. Am. Chem. Soc.*, 2010, **132**, 12690.
9. C. Y. Hong, X. Li and C. Y. Pan, *J. Mater. Chem.*, 2009, **19**, 5155.
- 10.(a) Y. L. Zhao, Z. X. Li, S. Kabehie, Y. Y. Botros, J. F. Stoddart and J. I. Zink, *J. Am. Chem. Soc.*, 2010, **132**, 13016.
- 55 (b) C. Wang, Z. X. Li, D. Cao, Y. L. Zhao, J. W. Gaines, O. A. Bozdemir, M. W. Ambrogio, M. Frascioni, Y. Y. Botros and J. I. Zink, *Angew. Chem. Int. Edit.*, 2012, **51**, 5460.
11. (a) P. Diez, A. Sanchez, M. Gamella, P. Martinez-Ruiz, E. Aznar, C. de la Torre, J. R. Murguia, R. Martinez-Manez, R. Villalonga and J. M. Pingarron, *J. Am. Chem. Soc.*, 2014, **136**, 9116. (b) Q. Yan, H. J. Zhang and Y. Zhao, *ACS Macro Lett.*, 2014, **3**, 472.